Cobalt Nanoparticle Arrays made by Templated Solid-State Dewetting

Yong-Jun Oh, Caroline A. Ross, Yeon Sik Jung, Yang Wang, and Carl V. Thompson*

Self-assembled cobalt particle arrays are formed by annealing, which cause agglomeration (dewetting) of thin Co films on oxidized silicon substrates that are topographically prepatterned with an array of 200-nm-period pits. The Co nanoparticle size and uniformity are related to the initial film thickness, annealing temperature, and template geometry. One particle per 200-nm-period pit is formed from a 15-nm film annealed at 850 °C; on a smooth substrate, the same annealing process forms particles with an average interparticle distance of 200 nm. Laser annealing enables templated dewetting of 5-nm-thick films to give one particle per pit. Although the as-deposited films exhibit a mixture of hexagonal close-packed and face-centered cubic (fcc) phases, the ordered cobalt particles are predominantly twinned fcc crystals with weak magnetic anisotropy. Templated dewetting is shown to provide a method for forming arrays of nanoparticles with well-controlled sizes and positions.

Keywords:
- arrays
- cobalt
- dewetting
- self-assembly
- thin films

1. Introduction

Magnetic metal nanoparticle arrays have attracted considerable interest for applications in patterned magnetic recording media, as well as catalyst arrays for growing carbon or semiconductor nanotubes.[1–5] These applications ideally require large-area, low-cost nanoparticle arrays with controlled long-range order. Well-ordered nanoparticle arrays are typically made by ''top-down'' lithographic planar processing methods, but the formation of sub-50-nm features becomes increasingly difficult as the dimensions of the particles are reduced. As an alternative, chemical synthesis[6–8] can be used to obtain magnetic nanoparticles with dimensions of a few nanometers and above. These may be deposited on a substrate by spin-coating, droplet drying, dip-coating, or Langmuir–Blodgett methods, but the long-range order of these arrays is limited.

Nanoparticle arrays may also be made by the spontaneous dewetting (or agglomeration) of a poorly wetting metal film on a substrate. For example, thin Fe, Ni, or Co films deposited onto silica break down into island arrays upon annealing at temperatures of several hundred degrees Celsius.[9–11] These arrays consist of islands with a range of sizes and spacings, and the islands lack long-range order. Giermann and Thompson reported the fabrication of Au nanoparticle arrays by dewetting a thin metal film on a topographically patterned Si substrate at elevated temperatures.[12] The substrate topography templates the dewetting, thus leading to an array of Au nanocrystals formed within the pyramidal pits of the substrate, and oriented such that their cubic (111) planes are parallel to the facets of the pits. The templating effect was attributed to the local curvature of the film over the topography, which leads to grooving of the film at the edges of the pits, and its eventual separation into nanoparticles located within the pits. Ordered arrays of nanoparticles formed by templated dewetting would be useful as catalysts for the formation of ordered arrays of nanotubes, because the sizes and positions of the nanoparticles are stable under the high processing temperatures used for nanotube growth, unlike agglomerated particles on a smooth substrate. However, the templated dewetting technique has not been extended to metals other than Ni, and its application to

[*] Prof. C. A. Ross, Y. S. Jung, Dr. Y. Wang, Prof. C. V. Thompson
Department of Materials Science and Engineering
Massachusetts Institute of Technology
Cambridge, MA 02139 (USA)
E-mail: caross@mit.edu
Prof. Y.-J. Oh
Advanced Materials Science and Engineering Division
Hanbat University (Korea)

DOI: 10.1002/smll.200801433

NANO MICRO small

transition metals, including those with noncubic structures, may be particularly interesting.

Herein, we describe the use of templated dewetting to fabricate ordered ferromagnetic cobalt nanoparticle arrays. Cobalt clusters as well as thin films are known to exhibit hexagonal close-packed (hcp), face-centered cubic (fcc), and/or ε-Co structures depending on the processing techniques employed, which indicates that allotropic transformations are greatly affected by conditions such as pressure, temperature, and nanoparticle morphology.[14–17] The microstructure of the templated particles is investigated, including the crystallographic relationship between the nanoparticles and the facets of the pyramidal pits. The magnetic properties of the arrays are discussed in terms of the geometry, phase transformations, and crystal structure of the Co nanoparticles.

2. Results and Discussion

2.1. Morphology

First, we describe the dewetting behavior of Co films on smooth oxidized silicon substrates. Thin cobalt films begin to agglomerate above 600 °C, and the tendency to form well-rounded, uniform Co particles increases with an increase in the annealing temperature. Films annealed at 850 °C form an array of particles with an average size and spacing (derived from analysis of the scanning electron microscopy (SEM) images) that depends on the film thickness. Figure 1 shows the linear relationship between the average interparticle distance and the initial film thickness. This result is consistent with Kan and Wong's theoretical treatment of solid-state dewetting.[18] Dewetting of a thin polycrystalline film on a smooth surface is known to begin with the penetration of holes at grain boundaries or at their triple junctions.[19] Once the film surface contacts the substrate surface, the rim of the holes rapidly retracts through capillary-driven surface diffusion to leave behind fingers that eventually pinch off to reduce the surface energy of the system.[20,21] Kan and Wong proposed that the finger distance is linearly proportional to the initial film thickness, that is, $\lambda_m = 2\pi H/k_m\alpha$, where λ_m, H, k_m, and α are the wavelength of the film perturbation, film thickness, wave number, and contact angle, respectively.[17] Considering that the finger distance determines the interparticle distance, this equation indicates that there should be a linear correlation between the average interparticle distance and initial film thickness, as seen in Figure 1.

We now describe dewetting on topographically patterned substrates. Four different topographic templates were examined in this work. Each consisted of a 200-nm-period square array of inverted-pyramidal pits with (111) facets etched into a (100) silicon wafer. Templates A, B, and C differed in the width of the mesas surrounding the pits. The ratio of the pit diameter (edge-to-edge distance) to mesa width was 2.5, 3.6, and 5.7, respectively, so that template C had the narrowest mesas (Figure 2a). An additional template, G, had a silicon nitride layer overhanging the pits (Figure 2b).

Figure 3a and b show the surface of 15-nm films annealed at 600 and 850 °C, respectively, on template C. At 600 °C, the Co particles are poorly defined, but at 850 °C rounded Co particles are seen in the pits. Control of the substrate geometry is crucial to obtain one particle per pit. For large mesa widths, as shown in Figure 3c, the size uniformity of the particles in the pits deteriorates because the cobalt film on top of the mesa agglomerates separately and then coalesces into neighboring pits, which changes the particle size. For a 15-nm-thick cobalt film, the most uniform particle arrays were obtained at 850 °C in template C (Figure 3b), which is consistent with the results for an Au film.[12] To investigate the effect of the thickness of the Co film, samples with thicknesses ranging from 3 to 20 nm were deposited on template C and annealed at 850 °C. One particle per pit was obtained when the thickness of the film was greater than 13–15 nm. For thinner films, as shown in Figure 3d and e, particles occur on the cross-points of the mesas, and multiple particles may appear in the pits. The particles on top of the mesas show better uniformity at small film thicknesses.

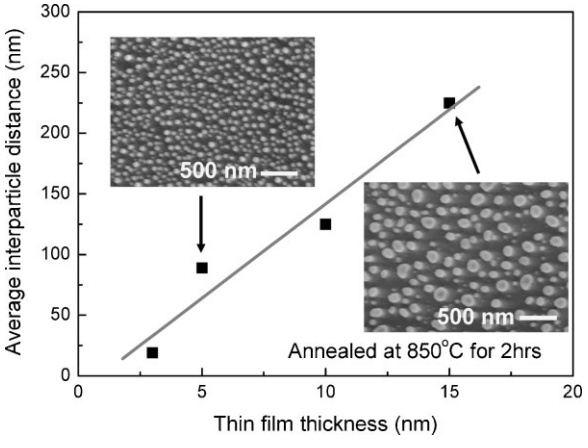

Figure 1. Average interparticle distance as a function of initial film thickness for Co films dewetted at 850 °C for 2 h on a smooth substrate.

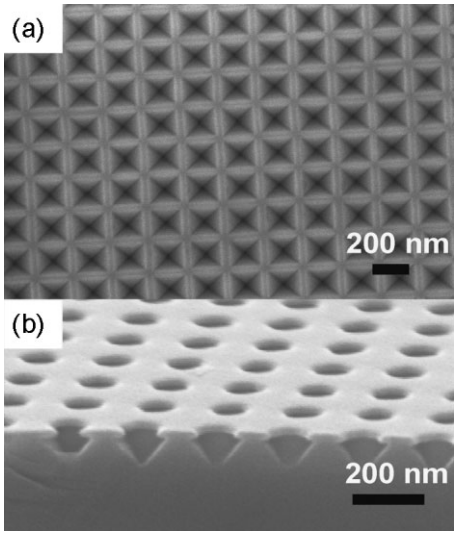

Figure 2. SEM images of a square array of inverted pyramids in (100) silicon. a) Template C (top view) and b) template G (cross-sectional view), in which the nitride layer can be seen overhanging the pits.

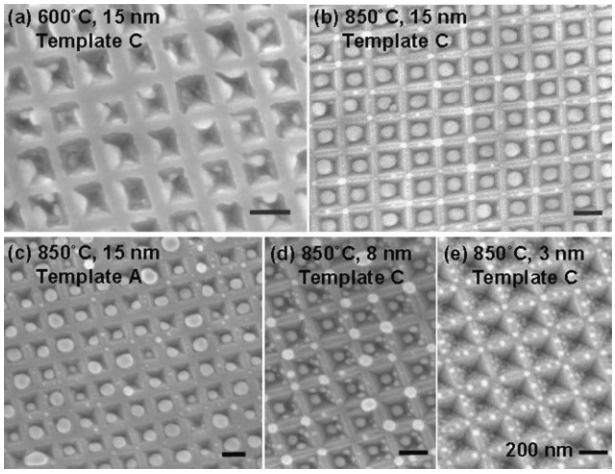

Figure 3. SEM images showing the appearance of dewetted Co films on patterned substrates on annealing at a) 600 and b–e) 850 °C. The samples shown in (a), (b), (d) and (e) were made by using template C (pit-to-mesa ratio ≈5.7) and the sample in (c) was made with template A (≈2.5). Co thickness: a–c) 15, d) 8, and e) 3 nm.

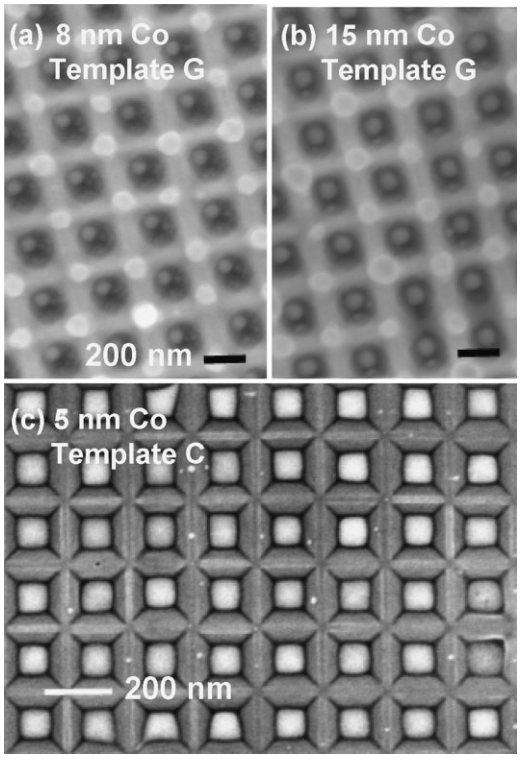

Figure 4. a,b) SEM images of 850 °C Co particles dewetted on template G. The initial film thicknesses were 8 and 15 nm, respectively. c) SEM image of a 5-nm Co film on template C, dewetted by laser annealing using a 266-nm-wavelength Nd–YAG laser with 100 pulses, each delivering 53 mJ cm^{-2} energy over a $5 \times 5\ mm^2$ area.

In this experiment, one particle per pit was formed at 850 °C for a film thickness of 15 nm on the 200-nm-period template. Interestingly, in Figure 1 a film thickness of 15 nm corresponds to an average interparticle distance of ≈200 nm when the film is dewetted on a smooth substrate. This suggests that the templating effect of the pit edges, which initiate instability of the film due to capillary-driven surface diffusion, would be effective in creating one particle per pit only when the period of the pits is smaller than the average interparticle distance on a flat substrate; when the period of the pits does not meet the above condition, the wavelength of the film perturbation (λ_m) in the pit becomes smaller than the pit dimension and multiple particles per pit would be expected to form. The concave inside corners and the apex of the pit will increase the agglomeration rate of a conformal film, due to the excess energy associated with the local curvature,[12,22] and may function as sites for multiple particle formation when the film thickness relative to the pit dimension is too small.

Figure 4a and b show the dewetted appearance of thin cobalt films deposited on template G, which includes a silicon nitride layer on top of the topographic template. For the same film thickness as template C, the particles are smaller and the size uniformity is much better than that of a film deposited on a template without a nitride layer. This is because the holes in the nitride layer limit the amount of Co within each pit.[13] The Co on the nitride also agglomerates into particles located at the cross-points of the porous nitride layer. The Co within the pits forms multiple particles for film thicknesses less than about 8 nm.

The range of film thicknesses that can produce one particle per pit on a given topography can be extended by the use of laser annealing instead of thermal annealing. Figure 4c shows a 5-nm-thick film agglomerated on template C through laser annealing. The sample was irradiated with 100 pulses of 266-nm light from a Nd–YAG laser. This process leads to particles of a larger size for a given film thickness compared to thermal annealing at 850 °C, very few particles on the mesas, and correspondingly better size uniformity of the particles within the pits. The microstructure and magnetic properties of laser-annealed arrays are reported separately below.

2.2. Microstructure

The microstructure of the 15-nm-thick as-deposited Co film on a smooth substrate is shown in Figure 5a, and the effect of thermal annealing at 500 °C is shown in Figure 5b and c. Transmission electron microscopy (TEM) reveals that the as-deposited film has 5- to 10-nm-diameter grains and consists of a mixture of hcp and fcc phases (see Figure 5d). This result differs from those of previous reports in which sputtered and electron-beam-evaporated films consist entirely of the hcp Co phase.[14,16,23] The cobalt crystal structure may be expected to depend on the processing technique, but it can be difficult to differentiate between hcp and fcc solely by X-ray diffraction because the peaks of the hcp and fcc Co phases occur at similar angles. In this work, high-resolution TEM clearly reveals the coexistence of the two phases. At 500 °C, a temperature too low to cause agglomeration, the TEM image shows an increase in grain size from 15 to 25 nm and a greater amount of the fcc Co phase (Figure 5e); however, some hcp Co phase still remains, thus showing an incomplete allotropic transformation from the hcp to the fcc Co phase.

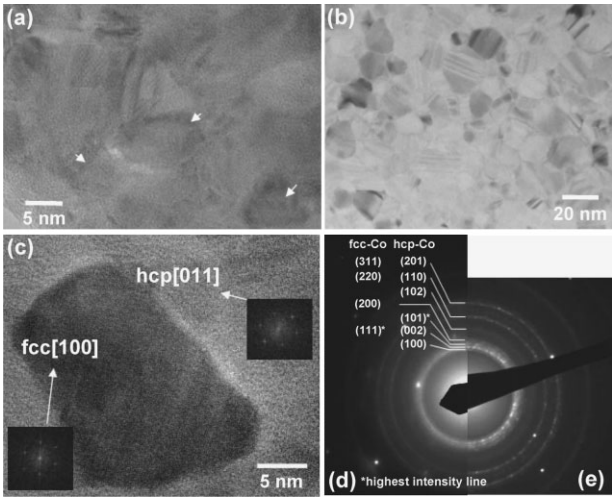

Figure 5. TEM images of a) an as-deposited film and b,c) a film annealed at 500 °C. The arrows in (a) indicate the fcc phase region of the [110] zone axis. d,e) Diffraction ring patterns for as-deposited films (d) and films annealed at 500 °C (e).

TEM images of particles dewetted at 850 °C from a 15-nm-thick film on templates C and G are shown in Figure 6a and b, respectively. The particles on both templates consist primarily of the fcc Co phase. The particles commonly exhibit twinning, but high-angle grain boundaries are rare. Figure 6a shows more than three twin variants in one particle (arrowed). The diffraction pattern (Figure 6c) shows rings, which indicates that there is no distinct biaxial crystal texture, unlike the case of Au where the close-packed (111) planes of the dewetted particles were parallel to the faces of the inverted pyramids.[12] Pole-figure analysis by X-ray diffraction confirms the lack of a preferred orientation in the Co crystals.

Figure 7 shows cross-sectional images before and after dewetting. The as-deposited conformal 15-nm-thick film consisted of grains 5 to 10 nm in diameter, which exhibit random crystal orientation. Dewetting leads to near-spherical particles that do not wet the apex of the pit. More than a quarter of the observed particles were oriented such that the (111) plane of the Co particle was approximately parallel to one pair of the inverted-pyramidal faces. For instance, in Figure 7b we can see the atomic images of the Co particle and silicon substrate at the same [110] zone axis, although the two crystals are tilted to some degree around the zone axis. This suggests that there is a tendency toward crystal reorientation to arrange the low-energy (111) fcc cobalt planes parallel to the silicon oxide-coated surfaces of the substrate during dewetting. However, the presence of multiple twinning, the incomplete transformation from hcp to fcc, and the near-spherical shape leading to small contact areas between the Co and the pit facets prevent development of a strong biaxial fcc crystallographic orientation, which explains the lack of preferred orientation seen in the X-ray data compared to the case of agglomerated Au.[12]

2.3. Magnetic Properties

Figure 8 compares the in-plane and out-of-plane magnetic hysteresis loops measured at ambient temperature for an as-sputtered 15-nm-thick Co film on template C, for films annealed at 500 and 850 °C to form arrays of nanoparticles. For comparison, the in-plane and out-of-plane loops of an as-deposited 15-nm-thick Co film on a flat surface are given in the inset of Figure 8a.

The as-deposited film on a flat substrate shows the expected strong in-plane magnetic anisotropy due to the shape of the film (hard axis saturation field = 2.5 kOe), a low in-plane coercivity of 6 Oe, and a saturation magnetization M_s close to that of bulk Co (1400 emu cm^{-3}). On the topographic template, the as-deposited film exhibits a similar M_s but a reduced anisotropy (hard axis saturation field ≈2 kOe) and a higher easy-axis in-plane coercivity of 330 Oe. These differences are attributed to the corrugation of the film, which reduces the net shape anisotropy and impedes domain wall motion.

The film annealed at 500 °C is still continuous, but as described above has a larger grain size and percentage of fcc grains than the as-deposited film. Magnetically, it shows lower anisotropy than the as-deposited film but a higher coercivity, both in-plane (570 Oe) and out-of-plane. These magnetic changes could result from the microstructural changes, an increase in the low-anisotropy fcc phase, and/or magnetoelastic effects in the film. For example, a tensile in-plane strain, coupled with the negative magnetostriction coefficient of Co, would lead to a magnetoelastic anisotropy normal to the film while a compressive strain would produce a contribution to in-plane anisotropy.

The 850 °C sample consists of an array of completely dewetted particles and shows very low anisotropy, with both the in-plane and out-of-plane loops having similar shapes. The low anisotropy is a result of the near-spherical shape of the particles and the presence of a primarily low-anisotropy fcc phase. Dipolar interactions between the particles, of order 50 Oe, are smaller than the coercive field and the array is therefore weakly interacting.

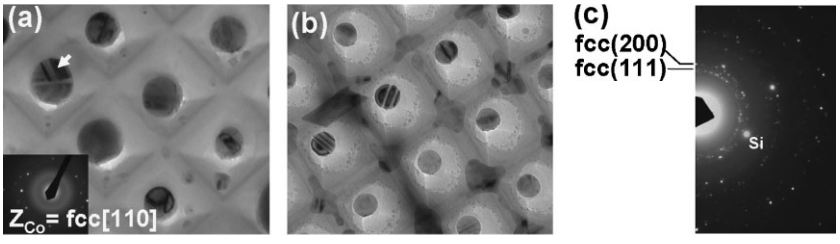

Figure 6. TEM plan-view images for Co particles on templates a) C and b) G. c) Diffraction pattern from the sample shown in (a). The particle indicated by an arrow in (a) shows multiple twins.

3. Conclusions

We have assembled ordered ferromagnetic cobalt nanoparticles on a topographically patterned SiO_2 template by the solid-state dewetting of a continuous thin film. The dewetting, or agglomeration, of

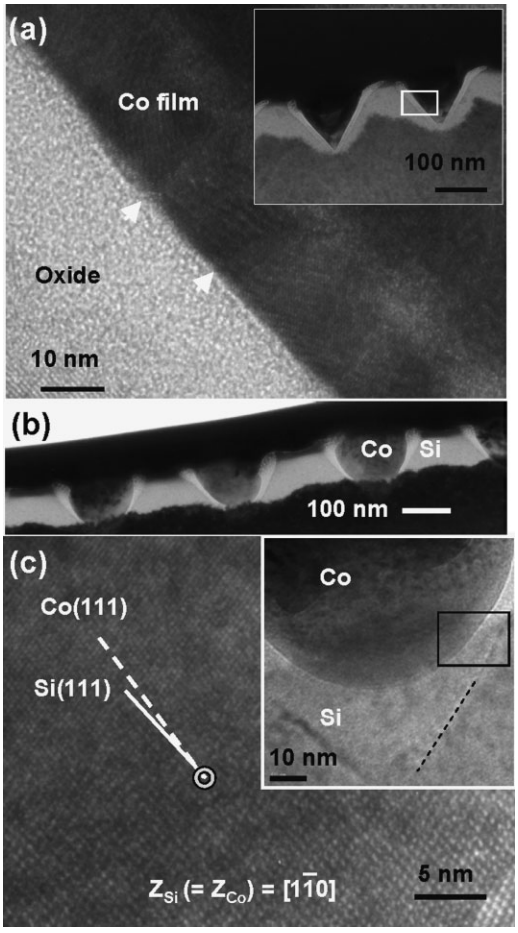

Figure 7. TEM cross-sectional images of a) an as-deposited 15-nm-thick film and b,c) the dewetted particles. b) Low-resolution image in which three rounded particles can be seen inside their pits. The Si appears bright, and the dark contrast at the top and bottom is from the sample preparation. c) High-resolution image of the particle shown in the inset. The pit facet is partly indicated with a dashed line. The rectangle in the top-right corner of the inset indicates the approximate location of the high-resolution image, which shows that the Co and Si share a zone axis.

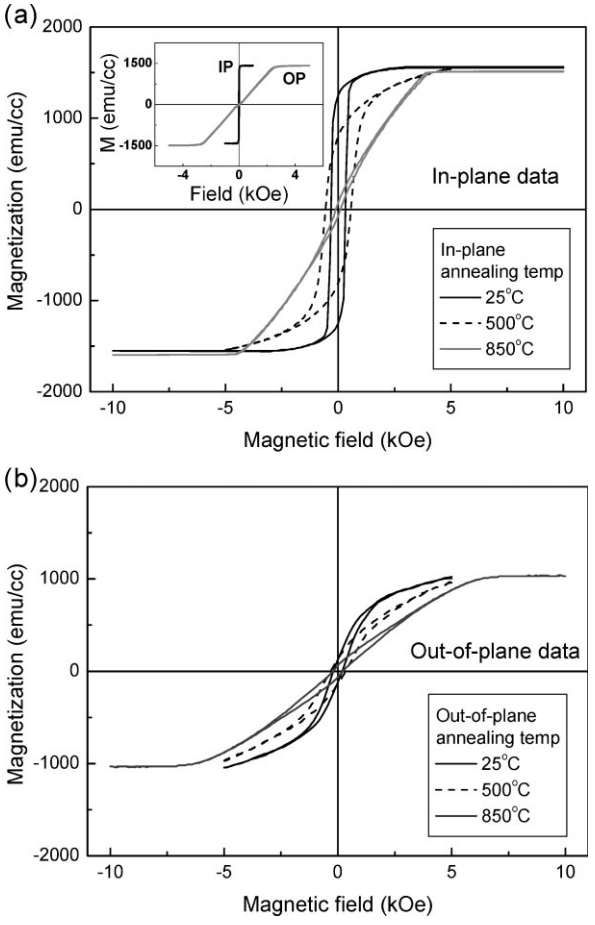

Figure 8. Magnetic hysteresis loops from 15-nm-thick Co films on template B after different annealing temperatures: a) in-plane and b) out-of-plane loops measured at room temperature. The inset in (a) is the hysteresis loop for a 15-nm-thick Co film on a smooth substrate.

the film on the topographic template is governed by capillary-driven surface diffusion of the film at the edges of the pits. The ordered topography can therefore lead to a microstructure in which one Co nanoparticle is located within each pyramidal pit.

On a smooth substrate, the average particle size and spacing increased linearly with film thickness, and the particle spacing was approximately 200 nm for a 15-nm-thick film annealed at 850 °C for 2 h. On the topographic substrate, one particle per pit was obtained when the pit dimension corresponded to the average distance between dewetted particles on a smooth substrate. A 15-nm film annealed at 850 °C therefore produced a well-defined array consisting of one rounded particle per pit on the 200-nm-period topography. Thinner films, however, produced multiple particles per pit. Laser annealing extends the range of film thicknesses that can produce one particle per pit for a fixed topography.

As-deposited films showed mixed fcc and hcp grains. Thermal annealing above 500 °C led to grain growth, with agglomeration becoming evident above 600 °C. After annealing at 850 °C, the agglomerated cobalt particles were mostly in the metastable fcc phase, and twins were common. The fcc phase is stable in Co at high temperatures (with an fcc-to-hcp transition temperature on cooling of 380 ± 12 °C[24]), and is retained on cooling the sample after annealing. The particles in the pits are approximately spherical, and do not wet the apex of the pit. At the locations where the particles contact the facets of the pits, there is often an alignment of the Co(111) planes with the pit facets. However, the presence of multiple twinning precludes a strong biaxial texture as seen for Au films agglomerated in similar pits.[12]

The collective magnetic behavior of an ordered Co particle array showed little anisotropy due to the low magnetocrystalline and shape anisotropy of the fcc Co and the lack of a strong crystallographic texture, and interactions between the particles were weak. A stronger magnetic anisotropy may be expected from templated agglomeration of an alloy that retains the hcp structure after annealing, or one in which twinning is suppressed.

small NANO MICRO

In conclusion, templated dewetting of Co films provides a route to the fabrication of ordered nanoparticle arrays in which both the size and location of the particles can be controlled. Such arrays may have applications in nanowire and nanotube catalysis, and ordered nanoparticle arrays made from Co alloys may be useful in magnetic data storage.

4. Experimental Section

The topographic templates consisted of 200-nm-period square arrays of inverted-pyramidal pits on (100) silicon wafers. Templates were made from (100) silicon wafers with a 40-nm-thick silicon nitride layer. After applying a negative photoresist (PR), the wafers were placed in an interference lithography system that used a 325-nm-wavelength laser beam to pattern the PR. Two perpendicular exposures of the laser standing wave yielded an irradiation dose sufficient to produce a square array of holes in the PR layer, with period controlled by the incidence angle of the laser. After creating holes in the PR layer by development, the holes were transferred to the silicon nitride layer and the PR layer was removed by reactive plasma-ion etching with CF_4 gas and subsequently O_2 gas. The wafer was etched in a solution of KOH (50 g) and deionized (DI) water (200 mL) at 40 °C for three different durations to form periodic pit arrays having different pit-to-mesa width ratios. After completely removing the nitride layer by immersion in concentrated HF solution for 10 min, the silicon was thermally oxidized at 800 °C for 1.5 h in dry air to grow a 12-nm-thick oxide layer. Each step included wafer cleaning with DI water and drying with N_2 gas. In particular, before thermal oxidation, the templates were cleaned and chemically oxidized by immersion in piranha solution for 10 min and then thoroughly rinsed in DI water. The resultant pit-to-mesa ratios were 2.5, 3.6, and 5.7 for templates A, B, and C, respectively. The inverted-pyramidal pit facets were parallel to the silicon (111) planes. A detailed procedure is described elsewhere.[12] We additionally fabricated an inverted-pyramid template G for which the silicon nitride layer was not removed prior to thermal oxidation. Cobalt films were deposited on the substrates by ion-beam sputtering and were subsequently annealed in forming gas ($N_2 + 4\%H_2$) for typically 2 h to induce dewetting. Laser dewetting was carried out by using a Nd–YAG laser of wavelength 266 nm, which produced 4-ns pulses of energy density 53 mJ cm^{-2} over an area of 5×5 mm^2 at a frequency of 10 Hz. Samples were laser annealed by using 100 laser pulses in an atmosphere of $N_2 + 4\%H_2$ flowing at 50 sccm. Magnetic measurements were made with a vibrating-sample magnetometer (to fields of 10 kOe) or an alternating-gradient magnetometer (up to 5 kOe). TEM cross-sectional samples were cut by a focused ion beam prior to imaging.

Acknowledgements

We thank Profs. H. I. Smith and K. Berggren for interference lithography facilities. This work was funded by the National Science Foundation, Division of Materials Research.

[1] B. D. Terris, T. Thomson, *J. Phys. D* **2005**, *38*, R199.
[2] C. A. Ross, *Annu. Rev. Mater. Sci.* **2001**, *31*, 203.
[3] M. Law, J. Goldberger, P. Yang, *Annu. Rev. Mater. Res.* **2004**, *34*, 83.
[4] M. Terrones, N. Grobert, J. Olivares, J. P. Zhang, H. Terrones, K. Kordatos, W. K. Hsu, J. P. Hare, P. D. Townsend, K. Prassides, A. K. Cheetham, H. W. Kroto, D. R. M. Walton, *Nature* **1997**, *388*, 52.
[5] J. Li, C. Papadopoulos, J. M. Xu, M. Moskovits, *Appl. Phys. Lett.* **1999**, *75*, 367.
[6] T. Hyeon, *Chem. Commun.* **2003**, 927.
[7] C. Petit, Z. L. Wang, M. P. Pileni, *J. Magn. Magn. Mater.* **2007**, *312*, 390.
[8] V. F. Puntes, K. M. Krishnan, P. Alivisatos, *Appl. Phys. Lett.* **2001**, *78*, 2187.
[9] H. Liu, G. Cheng, R. Zheng, Y. Zhao, C. Liang, *Surf. Coat. Technol.* **2008**, *202*, 3157.
[10] M. Chhowalla, K. B. K. Teo, C. Ducati, N. L. Rupesinghe, G. A. J. Amaratunga, A. C. Ferrari, D. Roy, J. Robertson, W. I. Milne, *J. Appl. Phys.* **2001**, *90*, 5308.
[11] Y. J. Yoon, J. C. Bae, H. K. Baik, S. J. Cho, S. J. Lee, K. M. Song, N. S. Myung, *Physica B (Amsterdam, Neth.)* **2002**, *323*, 318.
[12] A. L. Giermann, C. V. Thompson, *Appl. Phys. Lett.* **2005**, *86*, 121903.
[13] W. K. Choi, T. H. Liew, H. G. Chew, F. Zheng, C. V. Thompson, Y. Wang, M. H. Hong, X. D. Wang, L. Li, J. Yun, *Small* **2008**, *4*, 330.
[14] C. Cabral, Jr., K. Barmak, J. Gupta, L. A. Clevenger, B. Arcot, D. A. Smith, J. M. Harper, *J. Vac. Sci. Technol. A* **1993**, *11*, 1435.
[15] G. Mattei, C. Maurizio, C. de Julian Fernandez, P. Mazzoldi, G. Battaglin, P. Canton, E. Cattaruzza, C. Scian, *Nucl. Instrum. Methods Phys. Res. Sect. B* **2006**, *250*, 206.
[16] D. Kumar, A. Gupta, *J. Magn. Magn. Mater.* **2007**, *308*, 318.
[17] L. Chitu, Y. Chushkin, S. Luby, E. Majkova, A. Satka, J. Ivan, L. Smrcok, A. Buchal, M. Giersig, M. Hilgendorff, *Mater. Sci. Eng. C* **2007**, *27*, 23.
[18] W. Kan, H. Wong, *J. Appl. Phys.* **2005**, *97*, 043515.
[19] D. J. Sroloviz, S. A. Safran, *J. Appl. Phys.* **1986**, *60*, 247.
[20] E. Jiran, C. V. Thompson, *Thin Solid Films* **1992**, *208*, 23.
[21] H. Wong, P. W. Voorhees, M. J. Miksis, S. H. Davis, *Acta Mater.* **2000**, *48*, 1719.
[22] P. G. Shewmon, *Diffusion in Solids*, McGraw-Hill, New York 1963, p. 179.
[23] A. Sharma, S. Tripathi, R. Brajpuriya, T. Shripathi, S. M. Chaudhari, *J. Nanosci. Nanotechnol.* **2007**, *7*, 2041.
[24] J. Giber, R. Drube, V. Dose, *Appl. Phys. A* **1991**, *52*, 167.

Received: July 21, 2008
Published online: February 2, 2009

